Properties of the $\pi i_{13/2} \otimes \nu i_{13/2}$ band in odd-odd ^{184}Au

Y. H. Zhang,[1] Y. D. Fang,[1] G. de Angelis,[2,3] N. Marginean,[2] A. Gadea,[2] D. R. Napoli,[2] M. Axiotis,[2] C. Rusu,[2] T. Martinez,[2] H. L. Wang,[1] X. H. Zhou,[1] W. T. Guo,[1] M. L. Liu,[1] Y. X. Guo,[1] X. G. Lei,[1] M. Oshima,[4] and Y. Toh[4]

[1]*Institute of Modern Physics, Chinese Academy of Science, Lanzhou, China*

[2]*Istituto Nazionale di Fisica Nucleare, Laboratori Nazionali di Legnaro, Legnaro, Italy*

[3]*Hahn-Meitner-Institut, Berlin, Germany*

[4]*Japan Atomic Energy Research Institute, Tokai-mura, Ibaraki 319-1195, Japan*

(Received 17 July 2004; published 10 November 2004)

High-spin level structure in ^{184}Au has been reinvestigated using the multidetector array of GASP via the ^{159}Tb(^{29}Si, 4nγ)^{184}Au reaction at a beam energy of 140 MeV. The ground-state band and the excited $\pi i_{13/2} \otimes \nu i_{13/2}$ 2-qp band have been extended up to lower and higher spin states. An upbend has been observed in the excited band at $\hbar\omega \sim 0.25$ MeV and is interpreted as resulting from a pair of $\pi h_{9/2}$ alignment. This low-frequency $(\pi h_{9/2})^2$ alignment is supported by the measured $B(M1)/B(E2)$ ratios and alignment properties in neighboring odd-*A* nuclei. The linking transitions between the two bands and to the ground state have been established leading to a firm spin-and-parity assignment for the $\pi i_{13/2} \otimes \nu i_{13/2}$ band in ^{184}Au. This result provides strong evidence for the low-spin signature inversion in the $\pi i_{13/2} \otimes \nu i_{13/2}$ bands of odd-odd nuclei in the $A \sim 180$ mass region.

DOI: 10.1103/PhysRevC.70.057303 PACS number(s): 21.10.Re, 23.20.Lv, 27.70.+q

There has been a longstanding debate concerning the nature of first band crossing in the transitional Ir-Pt-Au nuclei. Usually, the first backbends observed in the high-spin yrast structure of deformed nuclei are attributed to the rotation alignment of a pair of high-*j* quasiparticles. For nearly the whole prolate rare-earth nuclei, this pair of high-*j* quasiparticle is thought to be the $i_{13/2}$ neutrons. In the Ir-Pt-Au region, however, the Fermi surface enters into the proton $h_{9/2}$ shell and the competition of the $(h_{9/2})^2$ proton alignment is expected. Based on the blocking arguments and the quasiparticle alignment properties, Larabee and co-workers [1] suggested that the upbends observed in ^{184}Pt and ^{185}Au below $\hbar\omega = 0.30$ MeV result from simultaneous alignments of the $(i_{13/2})^2$ neutrons and the $(h_{9/2})^2$ protons at degenerate frequencies. Furthermore, Janzen *et al.* [2] presented even stronger spectroscopic evidence [$B(M1)/B(E2)$ ratios] that both of these alignment processes occur below $\hbar\omega = 0.30$ MeV in ^{185}Pt and ^{183}Ir [2]. The $(\pi h_{9/2})^2$ alignment has also been proposed in several other nuclei such as in ^{186}Pt [3], ^{183,187}Au [4,5], and ^{186}Au [6]. However, the low-frequency $(\pi h_{9/2})^2$ alignment is not always supported by the cranked shell model calculations [7]. According to the theoretical scenario of Carpenter *et al.* [7], the $(\pi h_{9/2})^2$ alignment is only accepted in the bands of ^{185,186,187}Au involving an $i_{13/2}$ proton excitation, while it is unlikely to occur in even-even Pt because a negative γ deformation is predicted from TRS calculations. Recently, Robinson and co-workers [8] have measured the high-spin *g* factors in ^{180,182,184}Pt. It was concluded that the proton and neutron configurations are about equally important at high spin in the Pt isotopes near midshell.

Another interesting phenomenon is the low-spin signature inversion [9] which has been systematically observed throughout the chart of nuclides in the $\pi g_{9/2} \otimes \nu g_{9/2}$, $\pi h_{11/2} \otimes \nu h_{11/2}$, $\pi h_{11/2} \otimes \nu i_{13/2}$, and $\pi h_{9/2} \otimes \nu i_{13/2}$ configurations (see Refs. [10–12] and references therein) and has become an subject of many experimental [13,14] and theoretical [15] investigations. Noting the fact that the high-*j* intruder orbitals are involved in such signature-inversion bands, it is reasonable to expect the same phenomenon in the new $\pi i_{13/2} \otimes \nu i_{13/2}$ configuration. Although some indirect evidence has been reported in ^{176,178}Ir and ^{182}Au [16–20], however, the spin values had not been determined experimentally for any of the $\pi i_{13/2} \otimes \nu i_{13/2}$ bands. It is therefore still questionable to draw a definite conclusion that the low-spin signature inversion occurs in the $\pi i_{13/2} \otimes \nu i_{13/2}$ bands.

In order to gain an insight into the existing issues mentioned above, we have reinvestigated the high-spin band structures in the odd-odd ^{184}Au nucleus. Previously, the ground-state spin and parity of ^{184}Au have been determined to be 5^+ formed by the $\pi 3/2^-[532](h_{9/2}) \otimes \nu 7/2^-[514]$ configuration [21,22]. Ibrahim and co-workers [23] have observed the rotational bands built on the $\pi h_{9/2} \otimes \nu 7/2^-[514]$ and $\pi i_{13/2} \otimes \nu i_{13/2}$ configurations. Nevertheless, neither the expected low-energy γ transitions feeding the 5^+ ground state nor the interband transitions between the two bands have been observed [23].

High-spin states in ^{184}Au were populated via the ^{159}Tb(^{29}Si, 4nγ)^{184}Au reaction at a bombarding energy of 140 MeV. The ^{29}Si beam of 8 pnA was provided by the accelerator complex of the Tandem-XTU and ALPI at the Laboratori Nazionali di Legnaro, Italy, and focused onto a natural metallic ^{159}Tb foil of 2 mg/cm^2 thickness. The target was backed with gold of about 5 mg/cm^2 thickness in order to avoid the Doppler shift of emitting γ rays. In-beam γ rays were detected by the multidetector array of GASP, which consists of 40 Compton suppressed large volume Ge detectors and a multiplicity filter of 80 BGO elements. Events were collected when at least three suppressed Ge and two inner multiplicity filter detectors were fired. A total of 2.0×10^8 events was accumulated and sorted, after gain matching, into fully symmetrized matrices and cubes for off-line

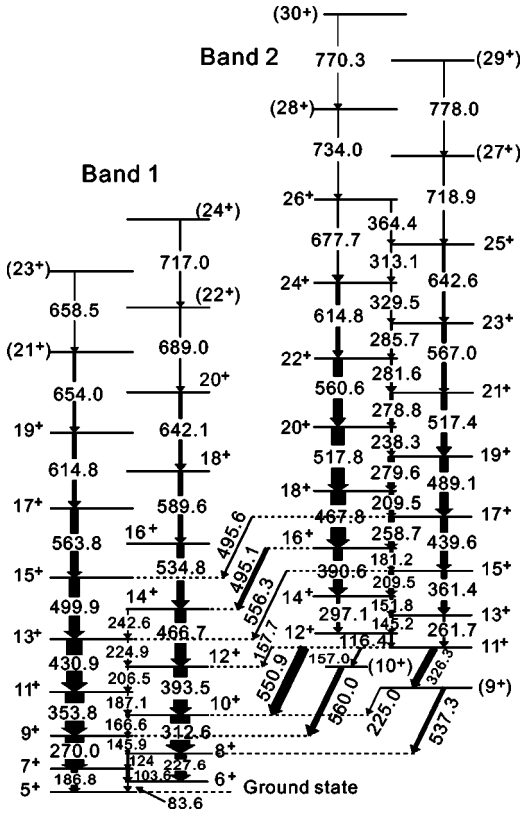

FIG. 1. Partial level scheme of ^{184}Au deduced from the present work. The width of arrows represents the intensity of decaying γ rays.

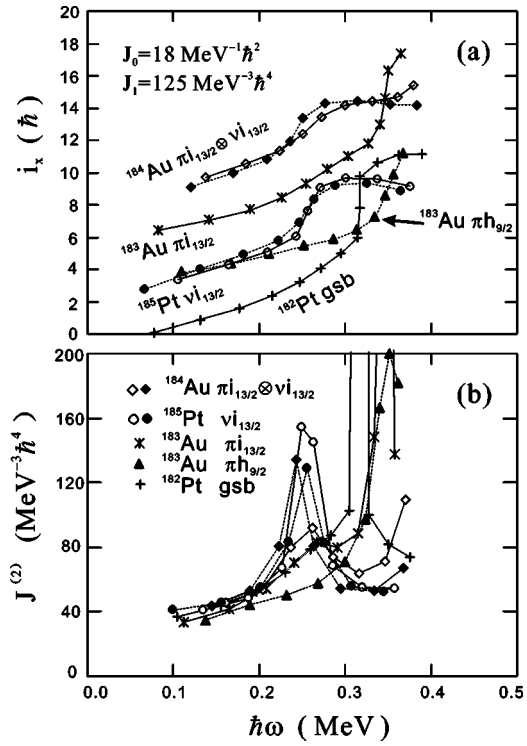

FIG. 2. Plot of (a) quasiparticle alignments i_x and (b) dynamic moment of inertia $J^{(2)}$ as a function of rotational frequency $\hbar\omega$. A common reference was used with Harris parameters indicated on the upper panel of the figure.

analyses. To determine the multipolarity of emitted γ rays, the coincidence events were sorted into an asymmetric matrix with one γ ray detected in one of the 12 detectors placed at 31.7°, 36°, 144°, and 148.3° (average angle is 34°/146°) and the other one detected in one of the 8 detectors at 90° with respect to the beam direction. The γ-ray intensities $I_\gamma(34°)$ and $I_\gamma(90°)$, used to determine the DCO ratios defined as $R_{DCO}=I_\gamma(34°)/I_\gamma(90°)$, were extracted from the coincidence spectra by setting gates on the 90° and 34° axes, respectively, of the above-mentioned asymmetric matrix. Setting gates on the stretched quadrupole transitions, $R_{DCO}(\gamma)$ values were close to unity for the stretched quadrupole transitions and $R_{DCO}\sim 0.5$ for the dipole ones.

From detailed analyses on the γ-ray coincidence relationships, a partial level scheme of ^{184}Au has been established and shown in Fig. 1. Comparing with the previous work of Ref. [23], the $\pi h_{9/2}\otimes\nu 7/2^-[514]$ ground-state band (band 1) and the $\pi i_{13/2}\otimes\nu i_{13/2}$ excited band (band 2) have been extended up to lower and higher spin states. Of most importance, we have identified two low-energy γ rays (83.6 and 186.8 keV) depopulating the previously reported 6^+ and 7^+ levels in the $\pi h_{9/2}\otimes\nu 7/2^-[514]$ ground-state band. These two γ rays are assigned as feeding directly the 5^+ ground state of ^{184}Au, leading to a firm spin-and-parity assignment for band 1. The interband connection is firmly established in this work due to observations of several linking transitions. The DCO ratio for the interband 551-keV transition was deduced to be 0.22 ± 0.02. This value is much smaller than that expected for the pure stretched dipole transitions. Then the 551-keV transition is assigned as a $\Delta J=1$, $M1+E2$ mixed transition with a negative $E2/M1$ mixing ratio. Consequently, the lowest member of band 2 can be assigned as 11^+. This assignment is also supported by the observation of a 495.1-keV, $E2$ transition [$R_{DCO}(495\text{ keV})=1.02\pm0.08$]. In addition, some other interband transitions and the extracted multipolarities provide supplementary arguments for the spin and parity assignments for band 2.

The aligned angular momentum i_x and dynamic moment of inertia $J^{(2)}$ versus rotational frequency $\hbar\omega$ are presented in Fig. 2 for the $\pi i_{13/2}\otimes\nu i_{13/2}$ band in ^{184}Au and the corresponding bands of neighboring nuclides [2,4,24]. A common reference with Harris parameters $J_0=18\hbar^2$ MeV^{-1}, $J_1=125\hbar^4$ MeV^{-3} has been subtracted in order that the ground-state band of ^{182}Pt [24] has a constant alignment after the first band crossing. As is clear in Fig. 2(a), an initial alignment as high as $\sim 10\hbar$ at $\hbar\omega=0.20$ MeV has been observed for the $\pi i_{13/2}\otimes\nu i_{13/2}$ band in ^{184}Au. This is consistent with the configuration assignment and the additivity property of alignment in the cranked shell model, that is, the $i_{13/2}$ proton contributes more than $6\hbar$, while the rest originates from the $i_{13/2}$ neutron. A sharp rise in alignment at $\hbar\omega\sim 0.32$ MeV is clearly observed in the $\pi i_{13/2}$, $\pi h_{9/2}$ bands of ^{183}Au, and in the ground-state band of ^{182}Pt. This band crossing has been attributed to the so-called AB crossing of the $i_{13/2}$ neutron [4,24]. Of particular interest, an upbend is observed in the $\pi i_{13/2}\otimes\nu i_{13/2}$ band at $\hbar\omega\sim 0.25$ MeV with an alignment gain of $\Delta i_x\approx 5\ \hbar$. This band crossing can be more clearly demonstrated in the plot of $J^{(2)}$ versus $\hbar\omega$ as shown in Fig. 2(b)

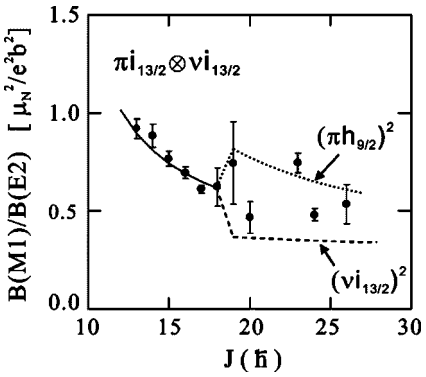

FIG. 3. Experimental and calculated $B(M1)/B(E2)$ ratios for the $\pi i_{13/2} \otimes \nu i_{13/2}$ band in ^{184}Au. The semiclassical predictions of Dönau and Frauendorf [25] assuming extra $(\pi h_{9/2})^2$ and $(\nu i_{13/2})^2$ alignments are shown as the dotted and the dashed line, respectively.

where a peak in $J^{(2)}$ at $\hbar\omega \sim 0.25$ MeV is observed. The crossing frequency is lower and the alignment gain is smaller comparing to the yrast band crossing in the even-even neighbors ^{182,184}Pt [7,24]. Given the fact that the neutron *AB* crossing is blocked in the $\pi i_{13/2} \otimes \nu i_{13/2}$ band, it is reasonable to attribute the observed band crossing to the alignment of a pair of $h_{9/2}$ protons, i.e., the proton *ef* crossing. The low-frequency $(\pi h_{9/2})^2$ alignment in the $\pi i_{13/2} \otimes \nu i_{13/2}$ band is consistent with the theoretical scenario of Carpenter *et al.* that the low-Ω $i_{13/2}$ proton drives the nucleus to a positive γ deformation ($\gamma \sim 10^0$) and quenches the proton pairing. Both factors favor the low-frequency $(\pi h_{9/2})^2$ alignment [7].

The low-frequency $(\pi h_{9/2})^2$ alignment in the $\pi i_{13/2} \otimes \nu i_{13/2}$ band of ^{184}Au can be examined by measuring the ratios of reduced transition probabilities $B(M1; I \rightarrow I-1)/B(E2; I \rightarrow I-2)$, which are much more sensitive to the quasiparticle configurations below and above the backbend. The experimental $B(M1)/B(E2)$ values are extracted from the measured branching ratios λ neglecting the $E2/M1$ mixing ratios (i.e., $\delta = 0$) since they enter into the $B(M1)/B(E2)$ calculations as $1/(1+\delta^2)$. The experimental $B(M1)/B(E2)$ values are compared in Fig. 3 with the theoretical calculations using the semiclassical expression of Dönau [25] and Frauendorf [6,26]. A reasonable set of parameters $\{i_n, g_{\Omega_n}, \langle\Omega_n\rangle, i_p, g\Omega_p, \langle\Omega_p\rangle, \langle K\rangle, g_R, Q_0\} = \{3.0, -0.30, 1/2, 6.0, 1.175, 9/2, 5.0, 0.30, 8.0\}$ was used in the calculations in order to well reproduce the $B(M1)/B(E2)$ values below backbend. For the high-spin levels, the theoretical results are shown for the assumption of (i) a $\nu i_{13/2}$ and (ii) a $\pi h_{9/2}$ crossing. As expected the two options result in opposite trends in the $B(M1)/B(E2)$ values after the crossing. The comparison between theoretical and experimental $B(M1)/B(E2)$ ratios shown in Fig. 3 leads to the conclusion that the observed band crossing is most likely due to the $(\pi h_{9/2})^2$ alignment.

A close inspection of Fig. 2 seems to reveal that there exists an extra crossing also in the $\pi i_{13/2}$ band of ^{183}Au and in the ground-state band of ^{182}Pt. This extra crossing is exhibited as a gradual alignment gain in i_x and a corresponding peak or a bump in $J^{(2)}$ at $\hbar\omega \sim 0.25$ MeV. If the $\pi h_{9/2}$ crossing is accepted in the $\pi i_{13/2} \otimes \nu i_{13/2}$ band of ^{184}Au, one may

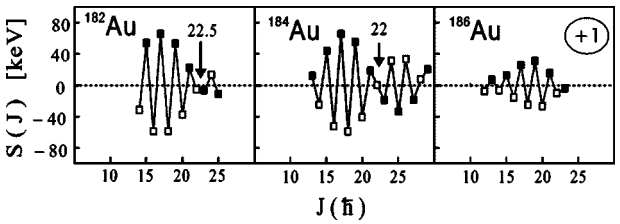

FIG. 4. Plot of signature splittings $S(J)$ vs J for the $\pi_{13/2} \otimes \nu i_{13/2}$ bands in ^{182}Au [19], ^{184}Au (present work), and ^{186}Au [6]. The level spins in the band of ^{186}Au are incremented by one unit in this plot. The arrow indicates the signature inversion spin.

suggest that the same $\pi h_{9/2}$ crossing is involved in both the $\pi i_{13/2}$ band of ^{183}Au and the ground-state band of ^{182}Pt. The $\pi h_{9/2}$ crossing in ^{183}Au has been proposed by Mueller and co-workers in Ref. [4]. Robinson and co-workers have measured the high-spin g factors in ^{180,182,184}Pt [24]. They suggested that proton and neutron configurations are about equally important at high spin in the Pt isotopes. The alignment features shown in Fig. 2 may be understood by assuming that both the $(\pi h_{9/2})^2$ and the $(\nu i_{13/2})^2$ alignments occur at degenerate frequencies near $\hbar\omega = 0.30$ MeV, with the $(\pi h_{9/2})^2$ alignment occurring first. A total alignment gain of more than $10\hbar$ provides further argument for the simultaneous $(\pi h_{9/2})^2$ and $(\nu i_{13/2})^2$ alignments.

With the spin and parity assignments for band 2, the typical level staggering curve $S(J) = E(J) - E(J-1) - \frac{1}{2}[E(J+1) - E(J) + E(J-1) - E(J-2)]$ versus spin J is plotted in Fig. 4 for the $\pi i_{13/2} \otimes \nu i_{13/2}$ bands in ^{182}Au [19], ^{184}Au (this work), and ^{186}Au [6]. The level spins are increased by one unit for the $\pi i_{13/2} \otimes \nu i_{13/2}$ bands in ^{186}Au comparing the level spacings in ^{184}Au and ^{186}Au. In such a plot, the points that have negative values are energetically favored over those with positive ones. The expected favored signature is $\alpha_f^{p-n} = \alpha_f^p + \alpha_f^n = \frac{1}{2} + \frac{1}{2} = 1$ for the $\pi i_{13/2} \otimes \nu i_{13/2}$ configuration. It can be seen in this figure that it is the unfavored-signature ($\alpha_{uf}^{p-n} = 0$) branch that is favored energetically at low and medium spins rather than the $\alpha_f^{p-n} = 1$ sequence. Such behavior has been referred to as the low-spin signature inversion [9]. With increasing angular momentum, the inverted signature splitting becomes decreasing, and the two signature branches cross with each other at $J_c = 22^+$ beyond which normal signature splitting is observed. The similar staggering pattern shown in Fig. 4 seems to suggest that the low-spin signature inversion occurs in the three $\pi i_{13/2} \otimes \nu i_{13/2}$ bands and the proposed level spins for ^{186}Au is reasonable. Another interesting feature, which is worthwhile noting, is that the signature splitting starts to become reinverted again beyond $J^\pi = 28^+$ in ^{184}Au. The level staggering pattern beyond the second signature inversion cannot be established because of the lack of higher-spin data; further experimental study is needed to confirm this phenomenon.

In conclusion, the high-spin band structures in odd-odd ^{184}Au have been reinvestigated using the ^{159}Tb(^{29}Si, $4n\gamma$)^{184}Au reaction and the multidetector array of GASP. The ground-state band $(\pi 3/2^-[532](h_{9/2}) \otimes \nu 7/2^-[514])$ and the excited $\pi i_{13/2} \otimes \nu i_{13/2}$ band have been extended up to lower and higher spin states. The in-band

$B(M1)/B(E2)$ ratios have been deduced and compared with theoretical calculations under the assumption of $(\nu i_{13/2})^2$ or $(\pi h_{9/2})^2$ alignment. The quasiparticle alignments and dynamic moment of inertia have been analyzed for the bands in ^{184}Au and the neighboring nuclei. These rotational properties can be coherently understood by invoking the low-frequency $(\pi h_{9/2})^2$ alignment below $\hbar\omega = 0.3$ MeV in the $\pi i_{13/2} \otimes \nu i_{13/2}$ band in ^{184}Au, the $\pi i_{13/2}$ band in ^{183}Au, as well as the ground-state band in ^{182}Pt. This conclusion is in agreement with the high-spin g-factor measurement in ^{180,182,184}Pt [27].

The spin and parity assignments for the $\pi i_{13/2} \otimes \nu i_{13/2}$ band in ^{184}Au have been established in this work based on the γ-spectroscopic method. Consequently the signature inversion is confirmed at low and medium spins. This may lead to a conclusion that the low-spin signature inversion occurs also in the $\pi i_{13/2} \otimes \nu i_{13/2}$ bands in $A \sim 180$ mass region.

The authors wish to thank the staffs in the LNL-INFN, Italy, for providing the ^{29}Si beam and their hospitality during experiment. This work is supported by the National Natural Sciences Foundation of China (Grant Nos. 10375077, 10025525, 10221003), the Major State Basic Research Development Program of China (Contract No. G2000077400), and the Chinese Academy of Sciences. Y.H.Z. acknowledges the CAS-INFN scientist exchange program.

[1] A. J. Larabee *et al.*, Phys. Lett. **169B**, 21 (1986).
[2] V. P. Janzen *et al.*, Phys. Rev. Lett. **61**, 2073 (1988).
[3] G. Hebbinghaus *et al.*, Z. Phys. A **328**, 387 (1987).
[4] W. F. Mueller *et al.*, Phys. Rev. C **59**, 2009 (1999).
[5] J. K. Johansson *et al.*, Phys. Rev. C **40**, 132 (1989).
[6] V. P. Janzen *et al.*, Phys. Rev. C **45**, 613 (1992).
[7] M. P. Carpenter *et al.*, Nucl. Phys. **A513**, 125 (1990).
[8] M. P. Robinson *et al.*, Phys. Lett. B **530**, 74 (2002).
[9] R. Bengtsson *et al.*, Nucl. Phys. **A415**, 189 (1984).
[10] L. L. Riedinger *et al.*, Prog. Part. Nucl. Phys. **38**, 251 (1997).
[11] G. García Bermúdez and M. A. Cardona, Phys. Rev. C **64**, 034311 (2001).
[12] Y. H. Zhang *et al.*, Phys. Rev. C **68**, 054313 (2003).
[13] M. A. Cardona *et al.*, Phys. Rev. C **59**, 1298 (1999).
[14] R. A. Bark *et al.*, Phys. Lett. B **406**, 193 (1997).
[15] F. R. Xu *et al.*, Nucl. Phys. **A669**, 119 (2000), and references therein.
[16] D. Hojman *et al.*, Eur. Phys. J. A **10**, 245 (2001).
[17] Y. H. Zhang *et al.*, Chin. Phys. Lett. **18**, 1323 (2001).
[18] Y. H. Zhang *et al.*, Eur. Phys. J. A **13**, 429 (2002).
[19] Y. H. Zhang *et al.*, Eur. Phys. J. A **14**, 271 (2002).
[20] R. A. Bark *et al.*, Phys. Rev. C **67**, 014320 (2003).
[21] F. Ibrahim *et al.*, Z. Phys. A **350**, 9 (1994).
[22] F. Le Blanc *et al.*, Phys. Rev. Lett. **79**, 2213 (1997).
[23] F. Ibrahim *et al.*, Phys. Rev. C **53**, 1547 (1996).
[24] D. G. Popescu *et al.*, Phys. Rev. C **55**, 1175 (1997).
[25] F. Dönau, Nucl. Phys. **A471**, 469 (1987).
[26] R. A. Bark *et al.*, Nucl. Phys. **A630**, 603 (1998).
[27] J. Nyberg *et al.*, Nucl. Phys. **A511**, 92 (1990).